Cell Stem Cell
Article

Discovery of Inhibitors of Microglial Neurotoxicity Acting Through Multiple Mechanisms Using a Stem-Cell-Based Phenotypic Assay

Susanne Höing,[1] York Rudhard,[2] Peter Reinhardt,[1] Michael Glatza,[1] Martin Stehling,[1] Guangming Wu,[1] Christiane Peiker,[2] Alexander Böcker,[2] Juan A. Parga,[3] Eva Bunk,[4] Jens C. Schwamborn,[4] Mark Slack,[2] Jared Sterneckert,[1,*] and Hans R. Schöler[1,5,*]

[1]Department of Cell and Developmental Biology, Max Planck Institute for Molecular Biomedicine, Röntgenstrasse 20, 48149 Münster, Germany
[2]Evotec AG, Manfred Eigen Campus, Essener Bogen 7, 22419 Hamburg, Germany
[3]Center for Research in Molecular Medicine and Chronic Diseases at the University of Santiago de Compostela, Avda. Barcelona, Santiago de Compostela s/n, E-15782, Spain
[4]Westfälische Wilhelms-Universität Münster, ZMBE, Institute of Cell Biology, Stem Cell Biology and Regeneration Group, Von-Esmarch-Strasse 56, 48149 Münster, Germany
[5]University of Münster, Medical Faculty, Domagkstrasse 3, 48149 Münster, Germany
*Correspondence: jsternec@mpi-muenster.mpg.de (J.S.), office@mpi-muenster.mpg.de (H.R.S.)
http://dx.doi.org/10.1016/j.stem.2012.07.005

SUMMARY

Stem cells, through their ability to both self-renew and differentiate, can produce a virtually limitless supply of specialized cells that behave comparably to primary cells. We took advantage of this property to develop an assay for small-molecule-based neuroprotection using stem-cell-derived motor neurons and astrocytes, together with activated microglia as a stress paradigm. Here, we report on the discovery of hit compounds from a screen of more than 10,000 small molecules. These compounds act through diverse pathways, including the inhibition of nitric oxide production by microglia, activation of the Nrf2 pathway in microglia and astrocytes, and direct protection of neurons from nitric-oxide-induced degeneration. We confirm the activity of these compounds using human neurons. Because microglial cells are activated in many neurological disorders, our hit compounds could be ideal starting points for the development of new drugs to treat various neurodegenerative and neurological diseases.

INTRODUCTION

Stem cells have the unique ability to both continually self-renew and differentiate into specialized cells. Pluripotent stem cells have the largest developmental potential because they are capable of differentiating into every somatic cell lineage as well as germ cells. For example, Wichterle and colleagues provided the first evidence for the efficient and direct generation of mouse embryonic stem cells (ESCs) into motor neurons (MNs; Wichterle et al., 2002). These cells were electrophysiologically functional and capable of restoring voluntary movement after transplantation into rats paralyzed by a viral infection that had killed their MNs (Deshpande et al., 2006). Multipotent stem cells have a more restricted differentiation potential, as they are capable of differentiating into a limited number of specialized cell types. For example, neural stem cells (NSCs) have the potential to differentiate into three cell types: neurons, astrocytes, and oligodendrocytes. By the expansion of stem cells in culture through their ability to self-renew followed by their directed differentiation into particular cell lineages, it is possible to obtain large numbers of stem cells that can be differentiated into a wide range of cell types in vitro whose function is comparable to that of primary cells. Such large quantities of specialized cells enable researchers to conduct new types of experiments into developmental biology as well as to test new possible therapeutic strategies that may lead to drug discovery.

The 21st century has seen a strong increase in the discovery of first-in-class drugs with new molecular mechanisms of action (MMOA), arising from phenotypic screening methodologies (Swinney and Anthony, 2011). In fact, between 1999 and 2008, the contribution of phenotypic screening to the discovery of first-in-class small molecule drugs exceeded that of target-based approaches; target-based approaches were the most successful for the discovery of follower drugs. Although primary cells would be the ideal cell type for phenotypic screening, the isolation of primary cells is extremely cumbersome, giving both low yields and heterogeneous results, making a high-throughput screening (HTS) campaign almost impossible. In addition, although cell lines are readily expandable, their phenotype is markedly different from that of primary cells, which makes their use in screening questionable. In contrast, stem cells can provide large numbers of homogeneous cells with a defined stage of differentiation and maturation (McNeish et al., 2010). Therefore, using stem cell technology, it is theoretically possible not only to construct disease models in vitro, but also to use these models to discover new drug candidates, representing a new paradigm for drug discovery.

Neurodegenerative diseases, such as amyotrophic lateral sclerosis (ALS), Parkinson's disease, and Alzheimer's disease,

are characterized by the progressive loss of specific types of neurons within the central nervous system. Increasing evidence indicates that abnormal activation of microglial cells, the resident immune cells of the central nervous system, plays an important role in the pathogenesis of neurodegeneration. Activation of microglial cells correlates well with the clinical pathology of neurodegeneration (Hall et al., 1998; Henkel et al., 2004; Kawamata et al., 1992; Turner et al., 2004). In a transgenic animal model of the motor neurodegenerative disease ALS, stimulation of microglial cells, such as with lipopolysaccharide (LPS), was found to exacerbate disease pathology, whereas inhibition of microglial activation increased survival (Kriz et al., 2002; Nguyen et al., 2004). On the other hand, microglial activation can have neuroprotective, rather than neurotoxic, effects. Under appropriate conditions, activated microglial cells secrete a mixture of neuroprotective factors, including brain-derived neurotrophic factor (BDNF), glial-cell-derived neurotrophic factor (GDNF), and neurotrophin-4 (NT4) (Hanisch and Kettenmann, 2007). Furthermore, microglial cells have been shown to influence the migration and differentiation of neural precursor cells (Aarum et al., 2003). Therefore, neurodegeneration associated with microglial activation is a complex phenotype with many different possible targets for new drug candidates. We postulate that a stem-cell-based assay is capable of recapitulating the spectrum of targets and effects that are therapeutically relevant to neurodegenerative diseases in humans.

We have developed a stem-cell-based model of motor neuron degeneration induced by microglial activation. This is an excellent model to demonstrate proof of concept for HTS for several reasons. First, although microglial cells have a significant role in many neurological disorders, their direct involvement in inducing neurodegeneration is probably best demonstrated in a transgenic mouse model of ALS (Boillée et al., 2006). As such, motor neurons are the most appropriate system for initial discovery of inhibitors of toxicity induced by microglial activation. However, such inhibitors could clearly be protective of other neuronal subtypes, as microglial activation is a hallmark of many neurodegenerative diseases. Second, the unique properties of stem cells enabled us to derive the large numbers of motor neurons needed for screening from a single batch of stem cells, which would not be possible with primary motor neurons, which are cumbersome to isolate and result in low yields. A true HTS using primary motor neurons would necessitate the usage of enormous-number batches of primary motor neurons, which is impractical. While neuronal cell lines are significantly more proliferative and, therefore, amenable to HTS, they have been shown to behave significantly differently from primary neurons (Czvitkovich et al., 2011). In contrast, ESC-derived motor neurons have been demonstrated to be functional and are even able to regenerate motor connections in paralyzed rodents, which demonstrates that their behavior mirrors that of primary motor neurons (Deshpande et al., 2006; Miles et al., 2004). Here, we report the generation of a stem-cell-based phenotypic assay that is suitable for HTS. We report on the discovery of compounds acting through multiple pathways, and confirm their activity using human neurons. We use in silico analysis to predict that our hit compounds are metabolically stable and able to cross both the intestinal epithelium and blood-brain barrier (BBB), which suggests that our hit compounds could be of interest in the development of therapeutic agents for many neurodegenerative and neurological diseases.

RESULTS

Assay Design and Development of HTS Platform

To enable HTS for microglial toxicity, we first developed a stem-cell-derived coculture system of astrocytes and MNs (Figure 1A). ESCs were derived from mice that contained a bacterial artificial chromosome (BAC)-based *Hb9-green fluorescent protein (GFP)* reporter vector (GENSAT GX229), which is expressed in postmitotic MNs (Figure S1 available online). These ESCs were expanded and differentiated into MNs (Figure S1), and were then isolated by fluorescence activated cell sorting (FACS). The differentiation medium and dissociation conditions were optimized for a maximal yield of highly GFP-expressing cells, which averaged 14% (Figure 1B). Gene expression analysis for *Islet-1* confirmed that these cells were indeed MNs (Figure 1B).

MNs are known to be dependent on trophic support for survival, and primary astrocytes are commonly used to sustain them in coculture. Although cortical astrocytes are available, directing the differentiation of NSCs into astrocytes is straightforward, efficient, and reproducible, and reduces animal handling and sacrifice. Therefore, astrocytes were differentiated from NSCs. On day 4 of differentiation, the astrocytes were seeded into Matrigel-coated 384-well plates. These astrocytes were then matured on-plate for increasing periods of time and tested for their ability to sustain MN survival after FACS. Fourteen days of maturation gave a robust MN survival after FACS isolation, which was used for further assay development and screening (Figure 1C). MN survival was quantified using high-content imaging for multiple readouts including total neurite length per well, total number of branch points per well, and total neurite area per well, based on the morphology of GFP-expressing MNs. Total neurite length per well resulted in the most favorable statistical significance, and we therefore used this readout throughout the remainder of the experiments. Although we expected to observe an initial increase in neurite length, we consistently observed a plateau effect for the first 4 days followed by significant cell death (Figure 1C). This is likely due to the fact that a single quantitative readout obtained for a well necessitated averaging all of these neurons, resulting in a plateau of total neurite length per well. Because the MNs have been isolated by FACS, they are under significant stress. Therefore, the cultures contain a mixture of stressed cells and healthy cells growing new axons. Similar curves were obtained for the other parameters.

The cell line BV2 was used as a source of microglial cells for several reasons. First, the isolation of primary mouse microglia is impractical for HTS. Second, microglial cells cannot yet be efficiently differentiated from an expandable stem cell source such as ESCs. Third, BV2 cells are well characterized and behave comparably to primary murine microglial cells with respect to stimulation and cell to cell interactions (Blasi et al., 1990). We tested the common stimuli interferon gamma (IFN-γ) and LPS for their ability to stimulate BV2 cells and found that the combination gave the most robust generation of nitric oxide (NO), which is indicative of microglial activation (Figure 1D). Therefore, we used BV2 cells stimulated with IFN-γ and LPS for further assay development and screening.

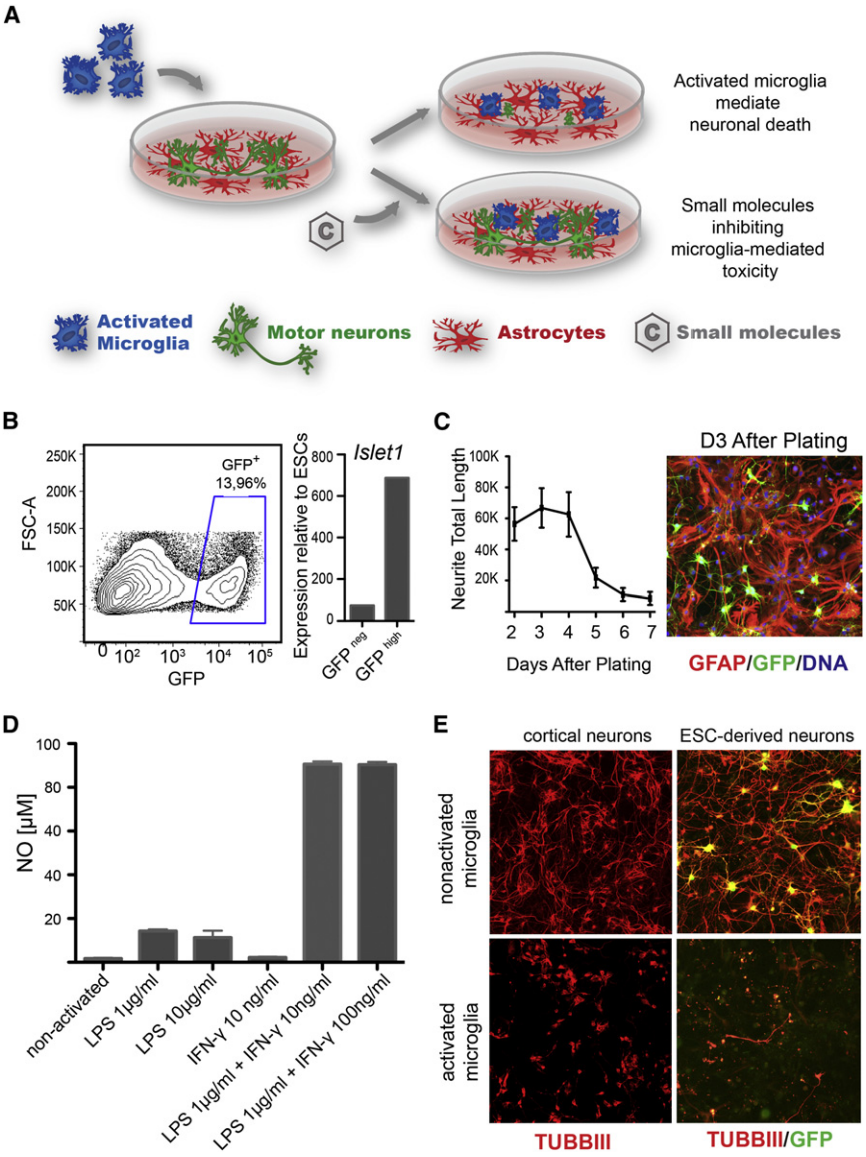

Figure 1. Development of HTS Platform

(A) Overview of the assay concept.

(B) Flow cytometric analysis of GFP induction by cultures of ESCs after 6 days of differentiation into MNs (left) and subsequent quantitative RT-PCR for *Islet1* expression (right).

(C) The astrocyte-MN coculture system: MN survival was evaluated at indicated days after FACS isolation and plating on astrocytes by high-content imaging using neurite total length per well as a readout (left), and a double fluorescent image (right) for Gfap immunostaining (astrocytes) and GFP (MNs).

(D) NO production after incubation of microglial cells with the indicated stimuli.

(E) Neurodegeneration induced by microglial activation for both cortical neurons (left) and unsorted ESC-derived neurons (right).

All data are shown as mean ± SD. See also Figure S1.

Finally, we evaluated the ability of IFN-γ and LPS-treated BV2 cells to induce MN death by introducing them in coculture with the MNs and astrocytes. We consistently observed MN death within 28 hr of introducing the activated BV2 cells. Cell death was not selective to MNs, as tested by costaining of the cells with βIII-tubulin (Figure 1E) and by using primary cortical neurons instead of stem-cell-derived MNs (Figure 1E). The coculture model was scaled down to a 384-well format and assessed with high-content imaging. The parameter neurite total length per well measured an average of 3,461 units (with a standard deviation of 1,208) and 41,149 (with a standard deviation of 5,543) when using activated and nonactivated microglial cells, respectively. This resulted in a z-value score of 0.46, which is indicative of a statistically robust assay.

Screening and Hit Profiling

To identify compounds that inhibited microglial toxicity, we screened more than 10,000 compounds at 10 μM screening concentration using the aforementioned phenotypic assay. These compounds were derived from several different libraries containing known drugs or novel chemical matter structurally enriched to target various different target groups. Active compounds were defined as compounds that increased the survival of MNs by at least 5 sigma above the mean of low control level (0%). Survival of MNs was defined as the total neurite length of all neurites of the MNs in the images captured from one well of the sample normalized to controls and expressed as a percentage. Thirty-seven active compounds were identified, representing a primary hit rate of 0.3% (Figures 2A–2C and Table S1). Through a structural similarity search, five of our primary hits were found to be related to compounds that had previously been described in the context of inflammation or neuroprotection (Table S2). To determine if this was significant, we repeated the similarity search with 37 randomly selected compounds. However, there was no overlapping target information. Based on these data, we conclude that there is a high likelihood that for 5 of 37 compounds there is a significant enrichment.

We next identified hits among the active compounds. A hit was defined as an active compound that produced a reproducible EC_{50}. We tested 34 of the 37 active compounds and identified 26 that showed a concentration-dependent and reproducible effect (Figure 3 and Table S1). The observed inhibition of microglia-mediated toxicity was not specific to MNs, as demonstrated by using cortical neurons instead of stem-cell-derived MNs (Figure 3). All experiments hereinafter were conducted with compound stocks that were repurchased from commercial vendors, and not from the original compound library supply. After reconfirmation of the repurchased compounds, a group

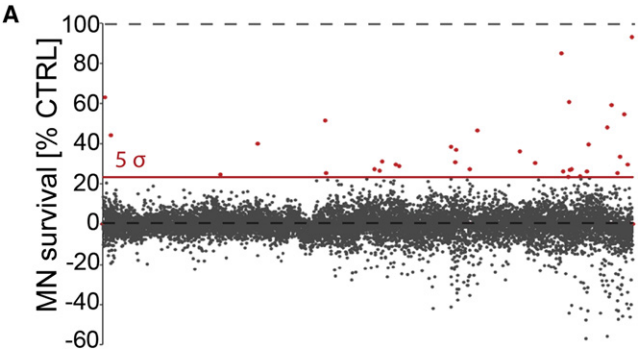

B

Library Subset	Total # Compounds	# Active Compounds	Rate [%]
CSB ACL	290	2	0.7
Carboxylic acids	12	0	0
Diverse islands	2,240	5	0.2
Evotec diverse	305	0	0
Ion channel	35	0	0
Kinases	986	2	0.2
Known Drugs	240	2	0.8
Others	7,142	23	0.3
Others (Oxford)	11	0	0
Pharma Focussed	408	3	0.7
Proteases	146	0	0
Protein Protein	4	0	0
Total	11,819	37	0.3

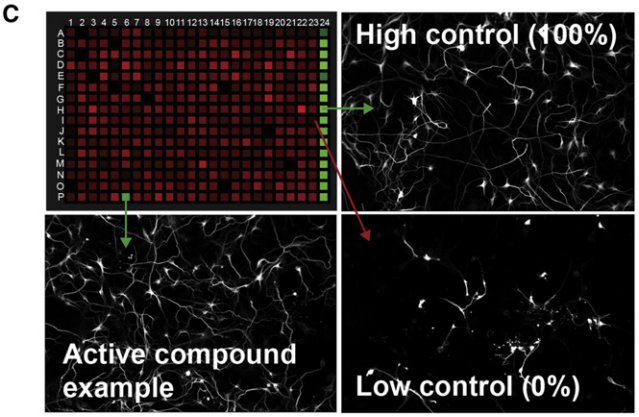

Figure 2. Identification of Active Compounds

(A) Summary of primary screening results shown as a dot plot of the normalized assay signal values of the primary screening consisting of 11,819 tested compounds. Active compounds, which increased MN survival by at least 5 sigma, are shown in red. MN survival was defined as the total neurite length of all neurites of the MNs in the images captured from one well of the sample normalized to the controls and expressed in percentages.

(B) List of library subsets and corresponding hit rates.

(C) Example plate from the primary screening, with 100% defined by the "High control (H)," which consisted of nonactivated microglial cells, and 0% defined by the "Low control (L)," which included activated microglial cells without any additional small molecules. An active compound example is also shown (well P6), showing 96% neuroprotection.

of 12 was selected for further testing. The results of representative hit compounds are shown in the sections below for each of the different orthogonal assays.

A prerequisite for animal testing is that the compounds be metabolically stable and able to cross both the intestinal epithelium and BBB. Previously, we developed in silico models that are predictive of these properties. For metabolic stability, we used a model that is predictive for being metabolized by cytochrome P450 (CYP), which is responsible for about 75% of drug metabolism (Guengerich, 2008). For each of the tested hits, there were no predicted metabolites, suggesting that they are stable against CYP-mediated degradation. Next, we assessed intestinal membrane permeability using an in silico model that is predictive for permeability across a layer of CACO-2 cells, which is currently the industry standard. Only two of the tested compounds, E29 and E34, were associated with a predicted log of apparent permeability (Papp) of less than −6, which indicates low permeability. All other compounds were predicted to be completely absorbed through the intestinal epithelium (Table S3). Finally, we used two different prediction methods to assess the potential of our hits to cross the BBB. Both predictions indicated that most of our hit compounds are able to cross the BBB (Table S3). Therefore, the hit compounds are generally predicted to be metabolically stable and bioavailable to neurons in the central nervous system, which are necessary attributes for future drug development.

Involvement of Microglial Cells in Neuroprotection by Hit Compounds

To further validate the hit compounds, we sought to determine the mechanism by which these compounds inhibited microglial toxicity. One of the identified hits (E34) is a known inhibitor of the nitric oxide synthase (NOS) L-NIO (Rees et al., 1990), and microglial activation is known to induce expression of NOS, which catalyzes the production of NO. Other hit compounds might similarly prevent microglial cells from producing toxic mediators such as NO. Alternatively, a hit might directly target MNs and protect them from NO-induced toxicity. To discriminate between these two modes of action, we substituted the activated microglial cells with 200 μM of the NO donor diethylenetriamine/nitric oxide (DetaNO), which efficiently induced MN death in our astrocyte-MN coculture system (Figure S2A). The results were directly compared with the effects of using activated microglial cells as toxic donors. If the hits inhibit microglial production of toxic agents such as NO, then they would not rescue MNs from DetaNO-induced death (Figure 4A). In contrast, hit compounds acting on microglia would be expected to rescue MNs from degeneration induced by activated microglial cells (Figure 4A). Of the tested compounds, this latter profile was observed for hit compounds E5, E14, E18, E19, E20, E21, E23, E25, E33, and E34 (Figures 4B and S2B). As expected, higher concentrations of hit compounds were usually toxic to MNs.

Next, we tested whether these hit compounds reduced NO production by microglial cells under activation conditions, and thereby protect (motor) neurons from degeneration. To test this, we measured the amount of NO production by activated BV2 cells in the presence of the hit compound using the Griess reaction (Figures 4C, 4D, and S2C). E5, E14, E19, E20, E25, E33, and E34 showed a dose-dependent decrease in NO production with EC_{50} values comparable with their EC_{50} values for MN rescue, which suggests that they inhibit production of toxic mediators by microglial cells.

However, it is also possible that the hit compounds might be selectively toxic to microglial cells, which would also reduce

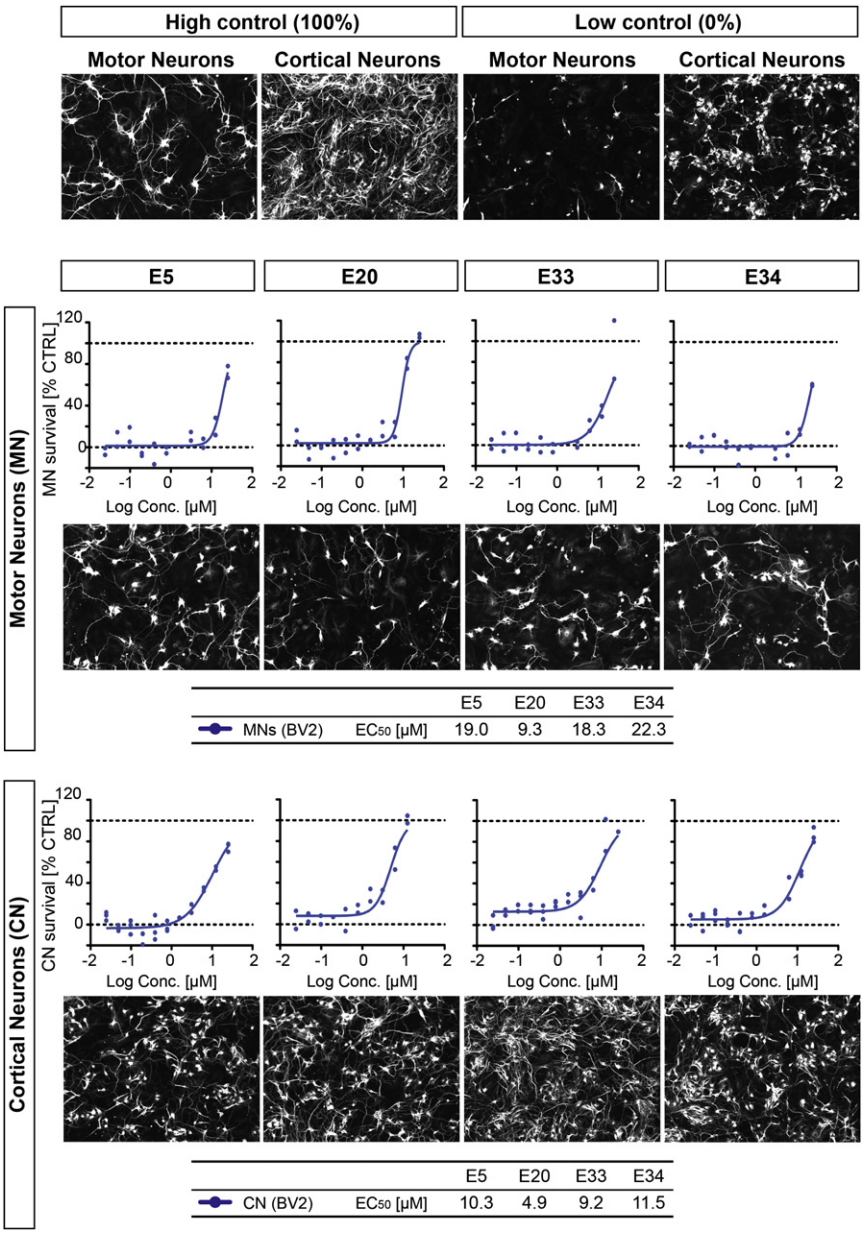

Figure 3. Identification of Hits

The neuroprotective effect and EC_{50} curves of four hit compounds (examples from the total of 26 hit compounds) are shown for both *Hb9*-GFP MNs (middle panel) and cortical neurons (lower panel). The respective EC_{50} values are listed in the embedded tables. Data are normalized to assay controls and constrained to 100%. Growth patterns of control conditions are also shown (top panel). For these data, compounds were assessed from the original screening library stocks.

NO production and protect MNs. To address this, we measured the cytotoxicity of the hit compounds by measuring the release of cytosolic lactate dehydrogenase (LDH; Figures 4C, 4D, and S2C). We found that E25 rescued the MNs by 80% and with an EC_{50} of 0.68 μM (Figure 4D). When tested alone, the efficiency of inducing microglial death was directly comparable to the inhibition of NO production (Figure 4D). Therefore, E25 prevents the degeneration of MNs by selectively killing microglial cells.

Hit Compounds Stimulate Transcription of Nrf2 Target Genes

To gain additional insight into the mode of action by hit compounds, we performed expression profiling. BV2 cells were activated in the presence of individual hit compounds for 4 hr and compared with BV2 cells activated without any additional compounds. Hierarchical clustering of the data revealed a tight association of the four hit compounds E5, E14, E19, and E20 (Figure 5A). For that reason, we then identified the genes that were upregulated in BV2 cells by all four of these hits compared with activated BV2 cells without any compound. Strikingly, we found a cluster of genes known to be targets of the transcription factor Nrf2 (Figure 5B). Likewise, our similarity search results already predicted that E14 would interact with Nrf2 (Table S1). These results suggested that Nrf2 activation is a possible mechanism for many of our hits. To test this, we examined the effects of two known activators of Nrf2—*tert*-butylhydroquinone (tBHQ) and bardoxolone (Bx)—in our MN protection assay (Figure 5C). As expected, both compounds protected MNs from degeneration. However, at higher concentrations, the compounds were neurotoxic, particularly Bx. Furthermore, as in our original hits, Bx did not rescue MNs from DetaNO-induced degeneration. Although tBHQ did rescue MNs from DetaNO-induced degeneration, it is likely that this is from an off-target effect, because tBHQ is known not to be specific to the Nrf2 pathway (Gharavi and El-Kadi, 2005).

Next, we used quantitative RT-PCR to assess the effects of our hit compounds on the transcription of known Nrf2 target genes in comparison with tBHQ and Bx. Because microglial cells were required for protection, we first examined BV2 cells. The genes *Gclm*, *Hmox1*, and *Nqo1*, which are known to be Nrf2 targets, were all upregulated after treatment with the hit compounds for as little as 2 hr (Figure 5D). Moreover, the overall time course of the upregulation of Nrf2 targets by our hit compounds was either comparable to or better than the upregulation induced by the positive-control compounds. Given the requirement of microglial cells for neuroprotection by our hit compounds, we also assessed the effects of our hit compounds on the transcription of Nrf2 target genes in both MNs and astrocytes (Figure 5E). In both cell types, our hit compounds induced upregulation of *Gclm*, *Hmox1*, and *Nqo1* comparably to or even

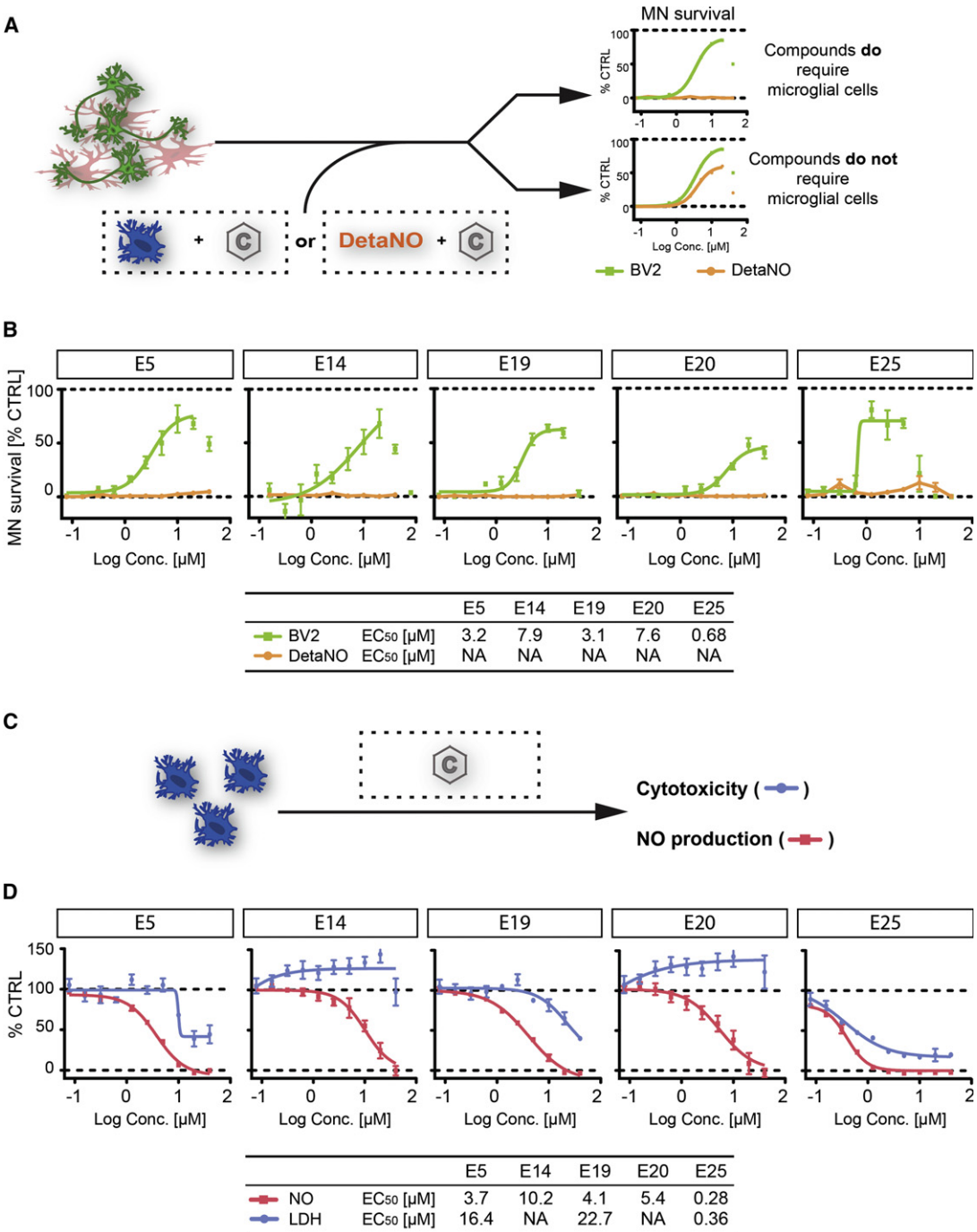

Figure 4. Involvement of Microglial Cells

(A) Experimental design to assess the necessity of microglial cells for neuroprotection by hit compounds. The astrocyte-MN coculture was treated for 30 hr with hit compound plus ether activated BV2 cells or DetaNO. Hits that depend on modulation of microglial cells for neuroprotection are expected to only rescue MNs from activated BV2 cells (green line), but not from DetaNO (orange line). In contrast, hits that are directly neuroprotective or act through astrocytes are expected to protect from both stress agents.

(B) MN survival was evaluated for the indicated hit compounds in the presence of either activated BV2 cells (green line) or with DetaNO (orange line).

(C) Activated BV2 cells were incubated with hit compounds for 30 hr and tested for NO production and LDH release.

(D) Dose-response curves for the indicated hits on BV2 cells for either the production of NO, indicating activation (red line), or the release of LDH, indicating cytotoxicity (blue line). The respective EC_{50} values are listed in the embedded tables. Data are normalized to assay controls and shown as mean ± SEM. The curves for NO production (red lines) are constrained to 0%.

NA = not applicable. In contrast to Figure 3, these data were obtained with compounds that had been repurchased. See also Figure S2.

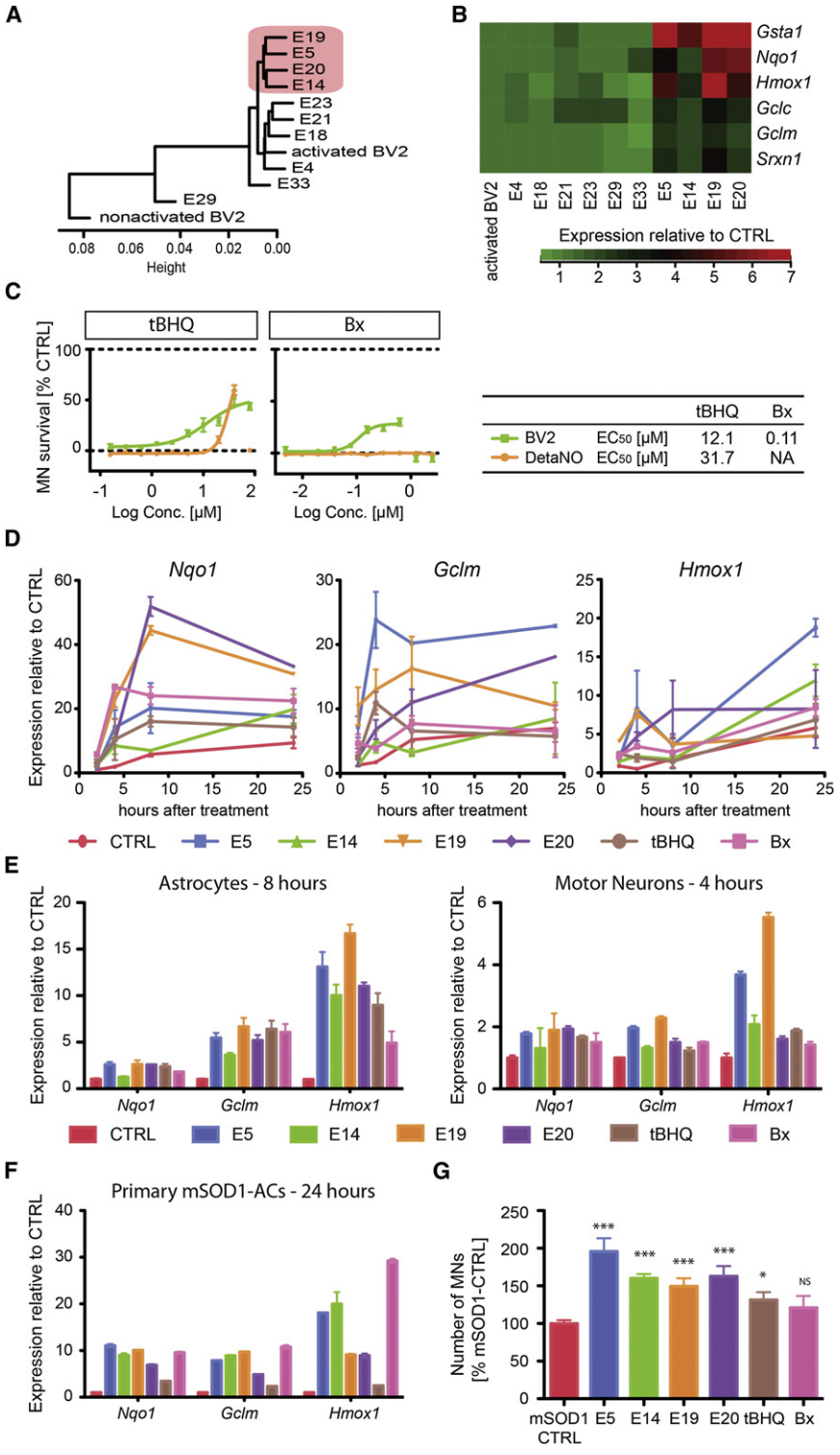

Figure 5. Hit Compounds Stimulate Nrf2 Target Gene Expression

(A) Hierarchical clustering of whole-genome expression data from nonactivated and activated microglial cells as well as activated microglial cells treated with individual hit compounds for 4 hr. The cluster of compounds E5, E14, E19, and E20 is highlighted (red box).

(B) Heat map from microarray data demonstrating upregulation of Nrf2 target genes by the hit compound cluster of E5, E14, E19, and E20. The color bar indicates gene expression normalized to activated BV2 control.

(C) Effect of known Nrf2 activators *tert*-butylhydroquinone (tBHQ) and bardoxolone (Bx) in the MN survival assay with activated BV2 cells (green line) or DetaNO (orange line). The experimental design is shown in Figure 4A. EC_{50} values are shown in the embedded table.

(D) Time course analysis of the expression of Nrf2 target genes by BV2 cells treated with the indicated compounds relative to nonactivated controls.

(E) Nrf2 target gene expression in astrocytes after 8 hr and MNs after 4 hr of treatment with the indicated compounds.

(F) Nrf2 target gene expression in G93A *SOD1* (designated mSOD1 in the figure) primary astrocytes after 24 hr treatment with the indicated compounds. Expression levels are normalized to those of untreated controls.

(G) Coculture of ESC-derived MNs with primary astrocytes expressing *SOD1* G93A (designated mSOD1 in the figure) in the presence of the indicated compound. The number of motor neurons after 3 days was quantified relative to that of untreated cultures.

All data are shown as mean ± SEM. NA, not applicable. Significance levels were determined using a two-tailed Student's t test. NS, not significant; $p > 0.05$; *$0.05 > p > 0.01$; **$0.01 > p > 0.001$; ***$p > 0.001$. qPCR statistics are listed in Table S4.

better than tBHQ and Bx. Interestingly, although Nrf2 is known to activate a detoxification pathway for reactive oxygen and nitrogen species including NO, the hits required microglial cells for a response. This suggests that Nrf2 modulates the activation state of microglial cells, which is supported by our previous observation that activated BV2 cells produce significantly less NO when treated with our hit compounds compared with controls. Interestingly, at least two studies confirm that Nrf2 inhibits microglial activation (Koh et al., 2009; Rojo et al., 2010). Our results show that, under our assay conditions, this additional role is more important for inducing neuroprotection than the classical antioxidant function of Nrf2.

It has been suggested that in ALS, astrocytes become reactive and secrete neurotoxic factors similar to microglial cells (Julien, 2007). Coculture experiments have demonstrated that primary astrocytes expressing *SOD1* G93A, which causes ALS pathogenesis in patients, secrete factors that are selectively toxic to MNs, including ESC-differentiated MNs (Nagai et al., 2007). It has also been suggested that modulation of *Nrf2* could be an effective treatment strategy for ALS. Specifically, treatment with small molecules

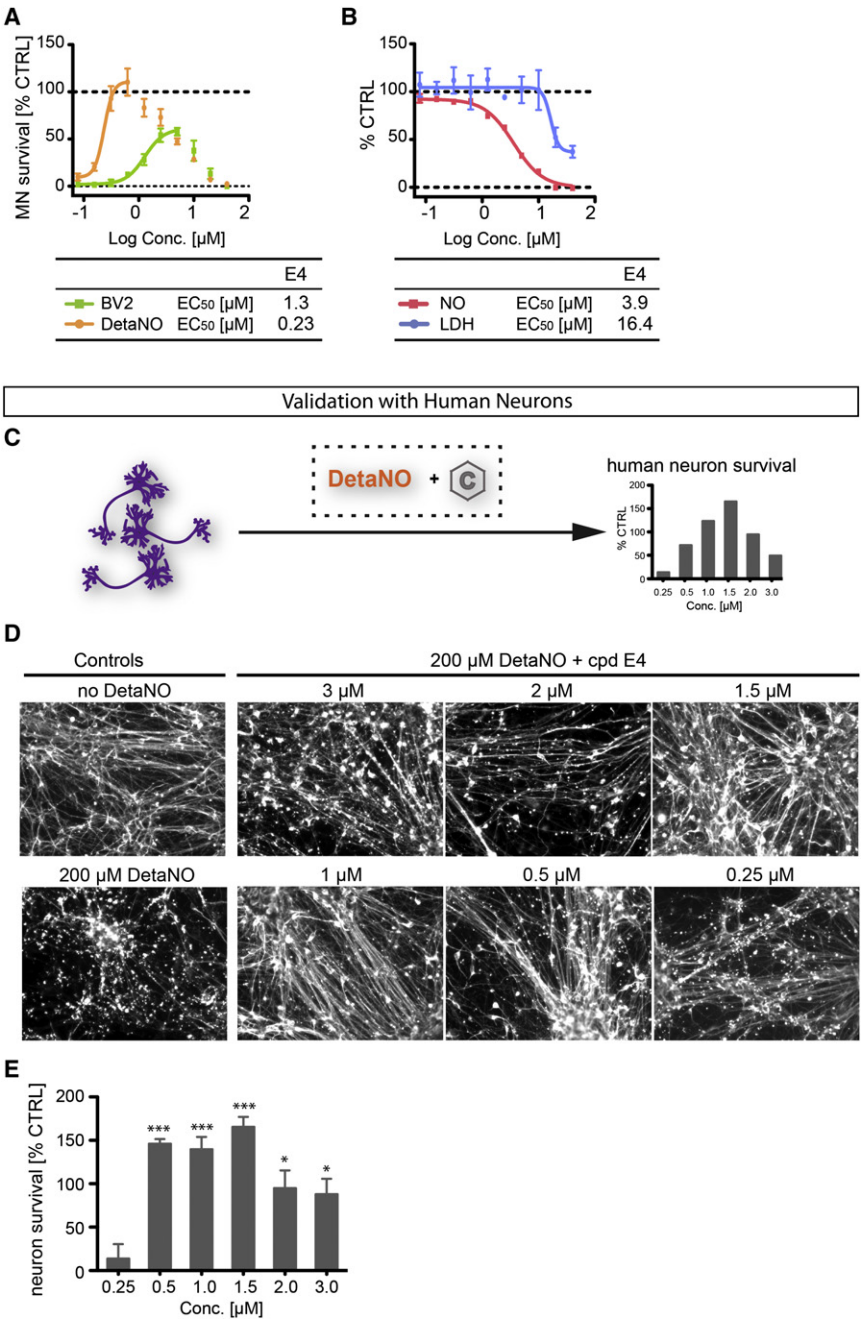

Figure 6. Protection from NO-Induced Cell Death by Hit Compound E4

(A) MN survival was evaluated for the indicated hit compound in the presence of either activated BV2 cells (green line) or with DetaNO (orange line).

(B) NO production (red line) and LDH release (blue line), indicating cell death, is shown for BV2 cells incubated with the hit compound E4 for 30 hr under activation conditions. Data are normalized to assay controls and shown as mean ± SEM.

(C) Experimental design for validation with human neurons. hNPC-derived neurons were treated with 200 μM DetaNO plus hit compound. Survival was analyzed by immunostaining for neurons (TUBBIII) after 72 hr of incubation.

(D) Validation of direct neuroprotection by E4 with human neurons.

(E) Quantification of human neuroprotection. Significance was determined using a two-tailed Student's t test. *0.05 > p > 0.01; **0.01 > p > 0.001.

See also Figure S3.

activating *Nrf2* and overexpression of *Nrf2* in astrocytes significantly extended survival of mice expressing transgenic mutant *SOD1* (Neymotin et al., 2011; Vargas et al., 2008). To test whether our compounds would be effective in this system, we isolated primary astrocytes from mice expressing transgenic G93A *SOD1*. We then exposed these primary astrocytes to E5, E14, E19, or E20 without any other stimulation. As expected, the hit compounds induced transcription of *Gclm*, *Hmox1*, and *Nqo1* comparably to or even better than the controls (Figure 5F). These results suggest that our hit compounds might rescue MNs from astrocyte-induced degeneration induced by primary astrocytes expressing mutant *SOD1*. We tested this by coculturing ESC-derived MNs with primary astrocytes expressing *SOD1* G93A in the presence of a hit compound for 3 days and then assessed the number of surviving motor neurons relative to untreated cocultures. We consistently observed a statistically significant increase in motor neuron survival in cultures treated with our hit compounds relative to control (Figure 5G). Consistent with our previous results, the increase in survival was greater with our hit compounds than with the positive controls tBHQ and Bx. These results indicate that E5, E14, E19, or E20 may be good starting points for novel drugs aimed at treating patients with ALS.

Direct Protection from NO-Induced Cell Death by Hit Compound E4

A significant advantage of our stem-cell-based screen is that it grants an ability to identify compounds acting on several different targets in a single assay. In contrast to the above hit compounds, which required microglial cells to induce neuroprotection, E4 protected MNs from DetaNO-induced degeneration with 100% efficiency (Figure 6A). Interestingly, the rescue by E4 was almost twice as potent with DetaNO-induced degeneration compared with activated microglia-induced degeneration (Figure 6A). In addition, the EC_{50} for DetaNO-mediated toxicity, 0.23 μM, was significantly lower than that for the microglia-mediated toxicity, 1.3 μM. These results demonstrate that E4 protects MNs directly from NO-induced degeneration and does not require the presence of microglial cells to exert neuroprotection.

To rule out the possibility that E4 induced uptake and "metabolization" of NO by astrocytes, we evaluated NO levels in the

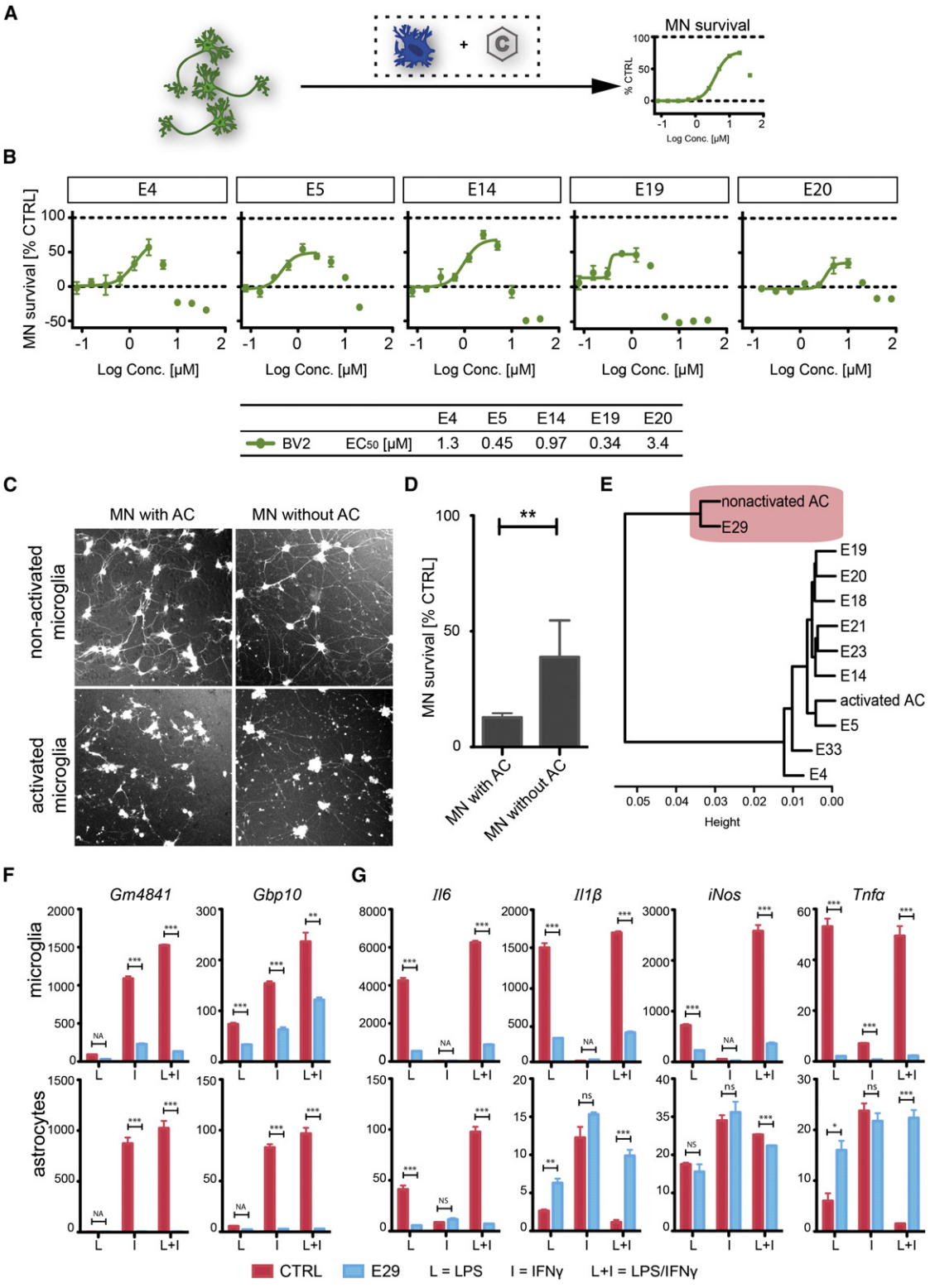

Figure 7. Role of Astrocytes in Neuroprotection

(A) Outline of the experimental procedure to assess the role of astrocytes. FACS-isolated MNs were cocultured with activated BV2 cells and hit compound, but without astrocytes. MN survival was analyzed after 30 hr.

(B) The dose-response curves for MN survival are shown for the indicated hit compounds. The respective EC_{50} values are listed in the embedded tables. Data are normalized to controls and shown as mean ± SEM.

presence of only astrocytes and no neurons. However, no significant effect was observed (Figure S3). These results also indicated that compound E4 did not chemically neutralize NO, in contrast to known NO scavengers such as 2-4-carboxyphenyl-4,4,5,5-tetramethylimidazoline-1-oxyl-3-oxide (Osiecki and Ullman, 1968). E4 also reduced the production of NO by activated microglial cells. The NO level in the presence of E4 was 16.5% compared to control, and the EC_{50} of this effect was 3.9 μM (Figure 6B). No significant cell death was observed at the EC_{50} concentrations, indicating that E4 did not induce the death of microglia (Figure 6B). This demonstrates that E4 not only inhibits the NO sensitivity of neurons, but also directly or indirectly inhibits the generation of NO in microglial cells. Given the limited information currently available on the biochemical function of E4, it is not possible to give mechanistic details about these dual functions within the same molecule.

For further validation, we used human neurons differentiated from human ESCs to assess neuroprotection of E4 from DetaNO (Figure 6C). As with the mouse neurons, 200 μM DetaNO induced the degeneration of human neurons. In contrast, E4 induced a dose-depended rescue of the human neurons from DetaNO (Figures 6D and 6E). These results correlated well with the increased survival rates of mouse MNs. Therefore, we conclude that E4 directly induces rescue of neurons, including human neurons, from NO-induced degeneration.

The Role of Astrocytes in Neuroprotection

Astrocytes play an important role in the pathology of ALS both in vitro and in vivo. To determine whether astrocytes are required for neuroprotection by hit compounds, we developed an astrocyte-free version of our microglial toxicity assay. FACS-isolated motor neurons were cultured in the presence of activated BV2 cells for 30 hr followed by quantification of MN survival using high-content imaging (Figure 7A). We consistently observed that all hit compounds tested were neuroprotective in the absence of astrocytes, which demonstrates that astrocytes are not required for neuroprotection (Figures 7B and S4). Because microglial cells are not required for E4 activity, we also tested for neuroprotection by E4 using FACS-sorted MNs and DetaNO. Consistent with previous results, neuroprotection was directly induced by E4 (Figure S4). As expected, all compounds demonstrated toxicity to MNs at high concentrations.

Although neuroprotection could be conferred in the absence of astrocytes by all tested compounds, we consistently observed a significant decrease in the toxicity of activated microglial cells when astrocytes were removed. In the original assay, which included astrocytes, after 30 hr there were virtually no MNs left (Figure 7C). Almost all neurites had degenerated under those conditions. In contrast, in the absence of astrocytes, 30 hr after coculture with activated microglial cells, many MNs still had neurites, signifying more moderate degeneration (Figure 7D). Taken together, these data suggest that astrocytes synergize with microglial cells and exacerbate MN degeneration.

Because primary astrocytes are known to become inflammatory under the same conditions that were used in our assay, we performed expression profiling of NSC-derived astrocytes under nonactivating and activating conditions. Interestingly, we observed that treatment of astrocytes with LPS and IFN-γ induced expression of inflammatory markers such as *Il6*, *Tnfα*, *iNos*, and *Stat1* (Figure S5A). As a result, we profiled the expression of astrocytes treated with hit compounds. Hierarchical clustering of the results demonstrated that hit E29 clustered significantly closer to the nonactivated astrocytes than to the activated astrocytes (Figure 7E). Analysis of the differentially expressed genes confirmed that E29 inhibited the induced expression of many inflammatory mediators in astrocytes activated by LPS and IFN-γ (Figure S5A). Because microglial activation is similar to astrocyte activation, we profiled the microglial cells activated in the presence of E29 and compared them with both nonactivated and activated BV2 cells (Figure S5B). E29 inhibited the induced expression of many inflammatory mediators in BV2 cells, although not to the same extent as in astrocytes. Assaying LDH release by astrocytes treated with E29 demonstrated that the observed decrease in the expression of inflammatory markers was not due to toxicity (Figure S5C).

Because E29 inhibited the activation of both astrocytes and microglial cells, we sought to determine if the compound acted by directly inhibiting either toll-like receptor 4 (Tlr4) or the IFN-γ receptor (Ifngr), which are the receptors for LPS and IFN-γ, respectively. We treated BV2 cells and NSC-derived astrocytes independently with LPS, IFN-γ, or both, and then performed quantitative RT-PCR for specific marker genes. In astrocytes and microglial cells, IFN-γ, but not LPS, specifically induced expression of *Gm4841* and *Gbp10* (Figure 7F). E29 inhibited the upregulation of both of these markers in response to IFN-γ. However, in BV2 cells, LPS specifically induced the expression of *Il1β*, *Il6*, *iNos*, and *Tnfα*, which was inhibited by E29 (Figure 7G). NSC-derived astrocytes induced less upregulation of *Il1β*, *iNos*, and *Tnfα* in response to LPS treatment compared with BV2 cells, which could be due to a variety of factors including maturation state. Therefore, taken together, our findings indicate that E29 inhibits both Tlr4- and Ifngr-induced transcription activation and is not specific to either one or the other.

DISCUSSION

Phenotype-based screens lead to the discovery of more first-in-class drugs than target-based approaches. Although primary cells would be the ideal reagent for phenotypic assays, primary cells, particularly from human patients, are unavailable in

(C) Fluorescent images showing *Hb9*-GFP MNs cultured with or without astrocytes (left and right panels, respectively), cocultured with nonactivated or activated microglia (lower and upper panels, respectively).
(D) Quantification of Figure 7C. Results are normalized to nonactivated, which was set as 100%.
(E) Hierarchical clustering of whole-genome data from nonactivated astrocytes, astrocytes activated with LPS and IFNγ, and activated astrocytes treated with the indicated hit compound for 4 hr. E29 clusters are close to the nonactivated control (red box).
(F and G) Expression analysis of IFN-γ-induced genes *Gm4841* and *Gbp10* (F) and LPS-induced genes *Il1β*, *Il6*, *iNos*, and *Tnfα* by microglial cells and astrocytes cultured under the indicated conditions.
Significances were determined using a two-tailed Student's t test. NS, not significant; $p > 0.05$; *$0.05 > p > 0.01$; **$0.01 > p > 0.001$; ***$p > 0.001$; NA, not applicable. See also Figures S4 and S5.

sufficient quantities and homogeneity for HTS. Transdifferentiation, which is induced by the expression of specific transcription factors, has been proposed as a possible alternative. However, induced transdifferentiation generally results in postmitotic cells that are incapable of clonal expansion, such as induced MNs (Son et al., 2011). Without expansion, transdifferentiation leads to the production of very limited numbers of cells that are not sufficient for screening. Stem cells, in contrast, are capable of significant expansion and differentiation into cell types that function comparably to primary cells. To further enable large-scale HTS, we have subsequently optimized an assay protocol that lacks the time-consuming FACS purification of motor neurons used in our pilot screen. Both protocols are detailed in the Experimental Procedures. Therefore, at present, stem cells offer an attractive alternative for phenotype-based screening. Our work provides powerful validation that this concept actually works.

Microglial activation and neuronal degeneration are hallmarks of many neurodegenerative diseases, including ALS, Huntington's disease, and Parkinson's disease. We have developed an assay to identify small molecules that inhibit neuronal degeneration induced by activated microglial cells. We demonstrated that it is possible to detect hits acting through multiple different pathways in a single assay. To discriminate between the different modes of action, we also developed secondary cell-based assays. For example, compound E4 both directly protected neurons from DetaNO toxicity and reduced microglial production of NO. We found that E25 reduced the production of neurotoxic compounds such as NO by inducing cell death in microglia. Another group of compounds modulated the activation of microglial cells, reducing the production of NO and thereby rescuing the neurons. We found that the four hit compounds E5, E14, E19, and E20 activated the Nrf2 pathway. Interestingly, these hits induced neuroprotection by modulating the activation state of microglial cells instead of directly inducing expression of detoxification genes in motor neurons. Activation of this pathway has previously been shown to be therapeutic in animal models of neurodegenerative diseases, including ALS, Parkinson's disease, and Alzheimer's disease (Jazwa et al., 2011; Li et al., 2012; Neymotin et al., 2011). This suggests that our hit compounds would be good starting points for new drugs treating a wide range of neurodegenerative diseases.

A significant challenge with cell-based phenotypic screenings will be determining the molecular target of the compounds. Target-based screens utilize biochemical assays with purified proteins. As such, it is very unusual to not know the intended target of the compound. In contrast, cell-based phenotypic screens are complex systems, and, as a result, the identified compounds will almost always require subsequent target deconvolution. Target deconvolution generally involves strategies such as pulldowns and siRNA testing, which are potentially time consuming and cumbersome. Given the relatively large numbers of hits that can be discovered in a phenotypic screen, such screening campaigns may need to involve fewer compounds than the traditional biochemical screens. Another strategy might be to first run pilot screens such as ours to determine a particular mechanism of interest and then focus larger screening efforts on that mechanism.

In conclusion, we report the generation of a stem-cell-based phenotypic assay that is suitable for HTS. We discovered small molecules acting in multiple and distinct pathways. In addition, we confirmed the activity of these compounds on human neurons. Considering that aberrant microglial activation is thought to play a role in multiple neurodegenerative disorders, the hits compounds identified here could be of interest in the development of therapeutic agents for multiple neurological diseases.

EXPERIMENTAL PROCEDURES

Screening Assay

HB9-GFP ESCs were derived from GENSAT mice [Tg(Mnx1-EGFP) GX229Gsat/Mmcd] carrying a transgenic BAC containing a GFP reporter under the control of the *HB9* promoter. The ESCs were maintained feeder-free in ESC medium and differentiated into MNs as described in Wichterle et al. (2002) with minor modifications. Embryoid bodies (EBs) were formed by plating single-cell ESCs on Petri dishes in DK10 medium. Starting on day 2, the medium was supplemented with 1 μM retinoic acid (Sigma-Aldrich) and 1 μg/ml purmorphamine (Alexis Biochemicals). On day 6 of differentiation, EBs were disaggregated. GFP-positive MNs were isolated by FACS and plated on either NSC-derived astrocytes or Matrigel (BD Biosciences)-coated 384-well plates as indicated. Alternatively, EBs were dissociated and plated on astrocytes without sorting by FACS. The astrocytes were generated from NSCs previously derived from Do et al. (2007). NSCs were differentiated with astrocyte medium containing 10% FCS. On day 4, the differentiating NSCs were replated on Matrigel-coated 384-well plates. The astrocytes were matured for 14 days. BV2 cells (Blasi et al., 1990) were activated with 1 μg/ml LPS (Sigma-Aldrich) and 10 ng/ml IFN-γ (PeproTech). As indicated, BV2 cells or DetaNO (Sigma-Aldrich) was added to the assay plates 1 day after the addition of MNs. Motor neurons were analyzed 30 hr after the addition of either BV2 cells or DetaNO using the Opera™ High Content Imaging and Analysis platform (Perkin Elmer) and the Arrayscan® VTI Live (Thermo Scientific, Cellomics). For quantification of images, the CSIRO Neurite Outgrowth evaluation module in an Acapella™-based script for Opera images, and the Cellomics Bioapplication Neurite Profiling for images from the Array Scan, both generating multiple readouts (including total neurite length and number of branch points) were used. Screening compounds were added simultaneously with the microglial cells or DetaNO. Each well (X) was normalized to internal plate controls [low control (L; 0%): activated BV2s or DetaNO, only DMSO; high control (H; 100%): nonactivated BV2s or no DetaNO, only DMSO] and expressed as a percent: MN survival [% CTRL] = (X − L)/(H − L)*100. Animal handling was conducted in accordance with the Max Planck and Evotec AG animal protection guidelines and the German animal protection laws. For additional details on cell derivation, culturing, differentiation, and screening, see Supplemental Experimental Procedures.

Human Validation Assay

Human neural precursor cells (hNPCs) were derived from human pluripotent stem cells (hPSCs) according to the modified protocol from Chambers et al. (2009) and propagation was performed similar to Koch et al. (2009). For details see Supplemental Experimental Procedures. For neuronal differentiation, hNPCs were seeded overnight on Matrigel-coated dishes in NPC expansion medium. Differentiation was initiated with NPC differentiation medium supplemented with 0.5 mM dibutyryl-cAMP. Screening was performed after 14 days of differentiation. See Supplemental Experimental Procedures for additional information.

Quantification of NO Production

NO was measured indirectly by detecting the degradation of the product nitrite (Griess assay; Green et al., 1982). Culture media was added to Griess reagent (Sigma-Aldrich) in a 1:1 ratio. After incubating at room temperature for 15 min, the absorbance was measured at 540 nm. Experimental values were corrected for background nitrite content in the media and calculated as percentage of controls.

Cytotoxicity Determination

Cytotoxicity was measured by the release of cytosolic LDH by dead and dying cells using the Cytotoxicity Detection Kit^{Plus} (LDH) (Roche Applied Science) according to the manufacturer's instructions and as detailed in the Supplemental Experimental Procedures.

RT-qPCR and Microarray Analysis

Cells for RNA isolation were lysed in the culture wells. Reverse transcription was performed with MMLV enzyme (USB) and oligo dT_{15} priming. qPCR was carried out using SYBR Green master mix (ABI). Calculations were based on the ΔΔCt method normalized to a housekeeping gene. Primer sequences used for subsequent confirmation studies are shown in Table S5. cDNA samples for global gene expression analysis were prepared with the linear TotalPrep Amplification Kit (Ambion). Hybridization on mouse-8 V2 chips (Illumina) was carried out as recommended by the manufacturer. Data analysis was done in Illumina genome studio and MS Excel.

ACCESSION NUMBERS

Microarray results are accessible at the GEO database under accession number GSE37611, in a MIAME-compliant format.

SUPPLEMENTAL INFORMATION

Supplemental Information for this article includes five figures, five tables, and Supplemental Experimental Procedures and can be found with this article online at http://dx.doi.org/10.1016/j.stem.2012.07.005.

ACKNOWLEDGMENTS

We are especially grateful to Rosario Donato for kindly providing the BV2 microglial cell line and to the GENSAT consortium for providing the *HB9-GFP* mice. Special thanks go to Rhea Brintrup, Kerstin Hergarten, Gisela Abt, and Katharina Moellmann for technical assistance; to Pierre Illouga for statistical analysis of screening data; to Annett Müller and colleagues for compound logistics; and to Arne Düsedau (HPI, Hamburg) for FACS. We would like to thank Fred Brookfield for assistance with SciFinder database searches and assessment of chemical structures. J.A.P. was funded by an Angeles Alvariño's fellowship (cofunded by the European Social Fund). We would also like to thank Areti Malapetsas for editing the manuscript. Y.R., C.P., A.B., and M.S. are employees of Evotech AG.

Received: October 18, 2011
Revised: April 30, 2012
Accepted: July 5, 2012
Published online: October 11, 2012

REFERENCES

Aarum, J., Sandberg, K., Haeberlein, S.L., and Persson, M.A. (2003). Migration and differentiation of neural precursor cells can be directed by microglia. Proc. Natl. Acad. Sci. USA *100*, 15983–15988.

Blasi, E., Barluzzi, R., Bocchini, V., Mazzolla, R., and Bistoni, F. (1990). Immortalization of murine microglial cells by a v-raf/v-myc carrying retrovirus. J. Neuroimmunol. *27*, 229–237.

Boillée, S., Yamanaka, K., Lobsiger, C.S., Copeland, N.G., Jenkins, N.A., Kassiotis, G., Kollias, G., and Cleveland, D.W. (2006). Onset and progression in inherited ALS determined by motor neurons and microglia. Science *312*, 1389–1392.

Chambers, S.M., Fasano, C.A., Papapetrou, E.P., Tomishima, M., Sadelain, M., and Studer, L. (2009). Highly efficient neural conversion of human ES and iPS cells by dual inhibition of SMAD signaling. Nat. Biotechnol. *27*, 275–280.

Czvitkovich, S., Duller, S., Mathiesen, E., Lorenzoni, K., Imbimbo, B.P., Hutter-Paier, B., Windisch, M., and Wronski, R. (2011). Comparison of pharmacological modulation of APP metabolism in primary chicken telencephalic neurons and in a human neuroglioma cell line. J. Mol. Neurosci. *43*, 257–267.

Deshpande, D.M., Kim, Y.S., Martinez, T., Carmen, J., Dike, S., Shats, I., Rubin, L.L., Drummond, J., Krishnan, C., Hoke, A., et al. (2006). Recovery from paralysis in adult rats using embryonic stem cells. Ann. Neurol. *60*, 32–44.

Do, J.T., Han, D.W., Gentile, L., Sobek-Klocke, I., Stehling, M., Lee, H.T., and Schöler, H.R. (2007). Erasure of cellular memory by fusion with pluripotent cells. Stem Cells *25*, 1013–1020.

Gharavi, N., and El-Kadi, A.O. (2005). tert-Butylhydroquinone is a novel aryl hydrocarbon receptor ligand. Drug Metab. Dispos. *33*, 365–372.

Green, L.C., Wagner, D.A., Glogowski, J., Skipper, P.L., Wishnok, J.S., and Tannenbaum, S.R. (1982). Analysis of nitrate, nitrite, and [15N]nitrate in biological fluids. Anal. Biochem. *126*, 131–138.

Guengerich, F.P. (2008). Cytochrome p450 and chemical toxicology. Chem. Res. Toxicol. *21*, 70–83.

Hall, E.D., Oostveen, J.A., and Gurney, M.E. (1998). Relationship of microglial and astrocytic activation to disease onset and progression in a transgenic model of familial ALS. Glia *23*, 249–256.

Hanisch, U.K., and Kettenmann, H. (2007). Microglia: active sensor and versatile effector cells in the normal and pathologic brain. Nat. Neurosci. *10*, 1387–1394.

Henkel, J.S., Engelhardt, J.I., Siklós, L., Simpson, E.P., Kim, S.H., Pan, T., Goodman, J.C., Siddique, T., Beers, D.R., and Appel, S.H. (2004). Presence of dendritic cells, MCP-1, and activated microglia/macrophages in amyotrophic lateral sclerosis spinal cord tissue. Ann. Neurol. *55*, 221–235.

Jazwa, A., Rojo, A.I., Innamorato, N.G., Hesse, M., Fernández-Ruiz, J., and Cuadrado, A. (2011). Pharmacological targeting of the transcription factor Nrf2 at the basal ganglia provides disease modifying therapy for experimental parkinsonism. Antioxid. Redox Signal. *14*, 2347–2360.

Julien, J.P. (2007). ALS: astrocytes move in as deadly neighbors. Nat. Neurosci. *10*, 535–537.

Kawamata, T., Akiyama, H., Yamada, T., and McGeer, P.L. (1992). Immunologic reactions in amyotrophic lateral sclerosis brain and spinal cord tissue. Am. J. Pathol. *140*, 691–707.

Koch, P., Opitz, T., Steinbeck, J.A., Ladewig, J., and Brüstle, O. (2009). A rosette-type, self-renewing human ES cell-derived neural stem cell with potential for in vitro instruction and synaptic integration. Proc. Natl. Acad. Sci. USA *106*, 3225–3230.

Koh, K., Cha, Y., Kim, S., and Kim, J. (2009). tBHQ inhibits LPS-induced microglial activation via Nrf2-mediated suppression of p38 phosphorylation. Biochem. Biophys. Res. Commun. *380*, 449–453.

Kriz, J., Nguyen, M.D., and Julien, J.P. (2002). Minocycline slows disease progression in a mouse model of amyotrophic lateral sclerosis. Neurobiol. Dis. *10*, 268–278.

Li, X.H., Li, C.Y., Lu, J.M., Tian, R.B., and Wei, J. (2012). Allicin ameliorates cognitive deficits ageing-induced learning and memory deficits through enhancing of Nrf2 antioxidant signaling pathways. Neurosci. Lett. *514*, 46–50.

McNeish, J., Roach, M., Hambor, J., Mather, R.J., Weibley, L., Lazzaro, J., Gazard, J., Schwarz, J., Volkmann, R., Machacek, D., et al. (2010). High-throughput screening in embryonic stem cell-derived neurons identifies potentiators of alpha-amino-3-hydroxyl-5-methyl-4-isoxazolepropionate-type glutamate receptors. J. Biol. Chem. *285*, 17209–17217.

Miles, G.B., Yohn, D.C., Wichterle, H., Jessell, T.M., Rafuse, V.F., and Brownstone, R.M. (2004). Functional properties of motoneurons derived from mouse embryonic stem cells. J. Neurosci. *24*, 7848–7858.

Nagai, M., Re, D.B., Nagata, T., Chalazonitis, A., Jessell, T.M., Wichterle, H., and Przedborski, S. (2007). Astrocytes expressing ALS-linked mutated SOD1 release factors selectively toxic to motor neurons. Nat. Neurosci. *10*, 615–622.

Neymotin, A., Calingasan, N.Y., Wille, E., Naseri, N., Petri, S., Damiano, M., Liby, K.T., Risingsong, R., Sporn, M., Beal, M.F., and Kiaei, M. (2011). Neuroprotective effect of Nrf2/ARE activators, CDDO ethylamide and CDDO trifluoroethylamide, in a mouse model of amyotrophic lateral sclerosis. Free Radic. Biol. Med. *51*, 88–96.

Nguyen, M.D., D'Aigle, T., Gowing, G., Julien, J.P., and Rivest, S. (2004). Exacerbation of motor neuron disease by chronic stimulation of innate

immunity in a mouse model of amyotrophic lateral sclerosis. J. Neurosci. *24*, 1340–1349.

Osiecki, J.H., and Ullman, E.F. (1968). Studies of Free Radicals. I. Alpha-Nitronyl Nitroxides a New Class of Stable Radicals. J. Am. Chem. Soc. *90*, 1078.

Rees, D.D., Palmer, R.M., Schulz, R., Hodson, H.F., and Moncada, S. (1990). Characterization of three inhibitors of endothelial nitric oxide synthase in vitro and in vivo. Br. J. Pharmacol. *101*, 746–752.

Rojo, A.I., Innamorato, N.G., Martín-Moreno, A.M., De Ceballos, M.L., Yamamoto, M., and Cuadrado, A. (2010). Nrf2 regulates microglial dynamics and neuroinflammation in experimental Parkinson's disease. Glia *58*, 588–598.

Son, E.Y., Ichida, J.K., Wainger, B.J., Toma, J.S., Rafuse, V.F., Woolf, C.J., and Eggan, K. (2011). Conversion of mouse and human fibroblasts into functional spinal motor neurons. Cell Stem Cell *9*, 205–218.

Swinney, D.C., and Anthony, J. (2011). How were new medicines discovered? Nat. Rev. Drug Discov. *10*, 507–519.

Turner, M.R., Cagnin, A., Turkheimer, F.E., Miller, C.C., Shaw, C.E., Brooks, D.J., Leigh, P.N., and Banati, R.B. (2004). Evidence of widespread cerebral microglial activation in amyotrophic lateral sclerosis: an [11C](R)-PK11195 positron emission tomography study. Neurobiol. Dis. *15*, 601–609.

Vargas, M.R., Johnson, D.A., Sirkis, D.W., Messing, A., and Johnson, J.A. (2008). Nrf2 activation in astrocytes protects against neurodegeneration in mouse models of familial amyotrophic lateral sclerosis. J. Neurosci. *28*, 13574–13581.

Wichterle, H., Lieberam, I., Porter, J.A., and Jessell, T.M. (2002). Directed differentiation of embryonic stem cells into motor neurons. Cell *110*, 385–397.